

# Surface Treatment of Polyimide Using Solid-source H<sub>2</sub>O Plasma for Fabrication of Ge Electrode

Mie Tohnishi,<sup>1\*</sup> Mina Sato,<sup>1</sup> Akihiro Matsutani,<sup>1</sup>  
Takashi Ubukata,<sup>2</sup> and Sachiko Matsushita<sup>3</sup>

<sup>1</sup>Semiconductor and MEMS Processing Division, Open Facility Center, Tokyo Institute of Technology,  
4259 Nagatsuta, Midori-ku, Yokohama 226-8503, Japan

<sup>2</sup>Department of Chemistry and Life Science, Graduate School of Engineering Science,  
Yokohama National University, 79-5 Tokiwadai, Hodogaya-ku, Yokohama 240-8501, Japan

<sup>3</sup>Department of Materials Science and Engineering, Tokyo Institute of Technology,  
2-12-1 Ookayama, Meguro-ku, Tokyo 152-8550, Japan

(Received December 5, 2022; accepted February 13, 2023)

**Keywords:** flexible semiconductor electrode, Ge, polyimide, H<sub>2</sub>O plasma, heterogeneous material adhesion

We demonstrated the surface treatment of polyimide using solid-source H<sub>2</sub>O plasma for the fabrication of Ge thin films as an electrode of flexible devices. By using the solid-source H<sub>2</sub>O plasma, the internal stress of a polyimide sheet with deposited Ge was decreased, and the adhesion between the polyimide and Ge was also improved. In addition, the solid-source H<sub>2</sub>O plasma treatment was effective for increasing the bending durability and decreasing the resistance of the Ge electrode on a polyimide surface. Moreover, we analyzed a polyimide surface treated with solid-source H<sub>2</sub>O plasma, by Fourier transform IR spectroscopy and X-ray photoelectron spectroscopy. We believe that the proposed solid-source H<sub>2</sub>O plasma process is useful for bonding between polyimide and Ge in the fabrication of flexible semiconductor electrodes.

## 1. Introduction

Recently, flexible electronic devices have been extensively studied because of their great potential in various applications, such as plastic flexible displays, electronic skin, flexible solar cells, and disposable printed electronics devices.<sup>(1)</sup> Also, a method for forming a semiconductor thin film with high carrier mobility on a flexible insulating substrate has been researched.<sup>(2–4)</sup> One of them is the formation of Ge electrodes on polyimide surfaces. Ge is one of the promising semiconductors that has been used for diodes, detectors, and energy conversion materials.<sup>(5–7)</sup>

Polyimide substrates have been used for the production of electronic devices and small lightweight wearable devices because polyimide has high mechanical strength, dimensional stability, wear resistance, heat resistance, and chemical resistance. Polyimide is a polymer with imide bonds in the main chain and is synthesized using polyamic acid, which is a product of the

---

\*Corresponding author: e-mail: [tohnishi.m.ab@m.titech.ac.jp](mailto:tohnishi.m.ab@m.titech.ac.jp)  
<https://doi.org/10.18494/SAM4276>

reaction between tetracarboxylic acid anhydride and oxydianiline upon high-temperature heating.<sup>(8)</sup>

However, in spite of its extensive usage and detailed characterization, the poor adhesion of metals to polyimide, which is a consequence of its low specific surface energy, must be overcome to render the fabricated devices flexible and reliable. The general polyimide–metal composites have limited adhesion strength, which is a key issue to be resolved currently. Hence, many researchers have studied the surface modification of polyimide for the purpose of improving its adhesion to metals.<sup>(9–12)</sup> Since flexible electronic devices may be used at various temperatures, the peeling and disconnection of electrodes might be induced by stress caused by the difference in the thermal expansion coefficient between the polyimide substrate and the electrode material. Therefore, the reduction of the internal stress of the polyimide sheet with deposited Ge and the adhesion between the polyimide and Ge are important issues.

There are many techniques for polymer surface modification. One is a wet process in which the polymer is modified in a chemical solution, and another is the dry process of plasma treatment.<sup>(13–19)</sup> A wet process has the environmental problem of the need to dispose the liquid waste. A dry process with O<sub>2</sub> and vapor H<sub>2</sub>O plasma is often used for bonding polyimide and metals.<sup>(20–22)</sup> However, vapor H<sub>2</sub>O plasma requires a high-pressure gas cylinder, a vaporizer, and a system for heating gas lines to avoid freezing due to the condensation of water vapor. To simplify such systems, a simple plasma source is necessary. Thus, we focused on solid-source H<sub>2</sub>O plasma treatment without a gas cylinder or vaporizer. In our previous work, we applied this plasma process to bond polydimethylsiloxane (PDMS) to a glass surface, and we demonstrated good adhesion between the two materials in the fabrication of a microchannel.<sup>(23)</sup> However, several properties of the adhesion between polyimide and electrode materials and the effect of heating on these properties have not been investigated.

In this work, we demonstrate the surface treatment of a polyimide surface using a solid-source H<sub>2</sub>O plasma treatment for the fabrication of Ge electrodes on a polyimide surface. In addition, we perform several characterizations of a Ge electrode on a polyimide surface: measurement of the warpage angle, measurement of the surface shape using an atomic force microscope (AFM), and evaluation of the adhesion characteristics by a bending test. In addition, the bonding mechanism between polyimide and a metal treated with solid-source H<sub>2</sub>O plasma is described on the basis of the results of analysis by Fourier transform IR spectroscopy (FTIR) and X-ray photoelectron spectroscopy (XPS).

## 2. Experimental Setup and Characterization Method

Figure 1 shows a schematic diagram of the solid-source H<sub>2</sub>O plasma system we made with a stainless-steel chamber and 23 mmϕ RF electrode (KXE-23, Kenix) for use in this experiment. The RF frequency is 13.56 MHz. A 30-mm-thick quartz top plate was placed on the stainless-steel chamber with an inner diameter of 300 mm. The RF electrode comprising of a metal container with an aperture diameter of 20 mm and containing 5 mL of water was placed in the chamber. The chamber was exhausted by a rotary pump. By evacuating the chamber, the water in the container loses its heat of vaporization and changes into solid ice. A polyimide sheet

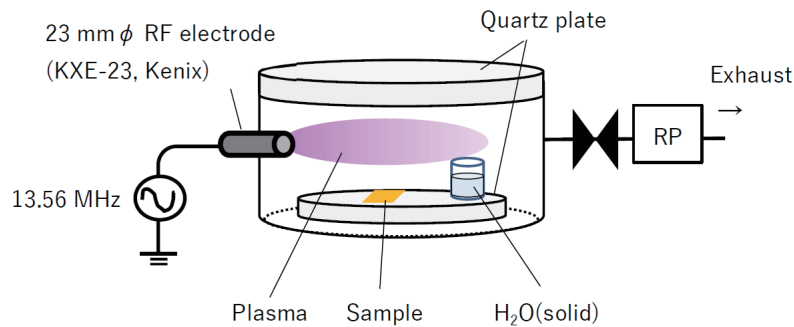


Fig. 1. (Color online) Schematic diagram of solid-source H<sub>2</sub>O plasma system.

(50- $\mu\text{m}$ -thick Kapton of DuPont) of  $20 \times 20 \text{ mm}^2$  was used as a sample. It was placed in the stainless-steel chamber. The process pressure was controlled by adjusting the conductance of the rotary pump.

The optical emission spectrum of the sample was measured with a spectrometer (Ocean Optics USB4000XR). The contact angle of the sample was evaluated by the  $\theta/2$  method using a drop of pure water. The surface roughness was measured using an AFM (AFM500II, Hitachi High-tech), and the depth of the crack in the bending test was measured using a Stylus Profiler (Dektak XT Bruker). To characterize the polyimide surface, FTIR (Spectrum II, Perkin Elmer) and XPS (PHI Versa Probe III, ULVAC phi) analysers were performed.

### 3. Experimental Results and Discussion

#### 3.1 Optical emission spectra of solid-source H<sub>2</sub>O plasma

Figure 2(a) shows a photograph of the solid-source H<sub>2</sub>O plasma observed through the top quartz plate of the chamber. Figure 2(b) shows an optical emission spectrum of the solid-source H<sub>2</sub>O plasma discharged at 10 W and 100 Pa. Several peaks associated with OH (308 nm), H (656 nm), and O (777 nm) are observed.

#### 3.2 Contact angle of polyimide surface after solid-source H<sub>2</sub>O plasma treatment

Figure 3(a) shows the contact angles of the polyimide surface before and after solid-source H<sub>2</sub>O plasma treatment. It was found that the contact angle was decreased by solid-source H<sub>2</sub>O plasma treatment. Figure 3(b) shows the contact angle of the polyimide surface after solid-source H<sub>2</sub>O plasma treatment as a function of storage time. The polyimide was stored in the plastic container in air. The contact angle of the polyimide surface decreased with decreasing process pressure, and it was  $17^\circ$  at a process pressure of 80 Pa. The decrease in the contact angle of the polyimide surface was maintained for at least 7 days after the solid-source H<sub>2</sub>O plasma treatment.

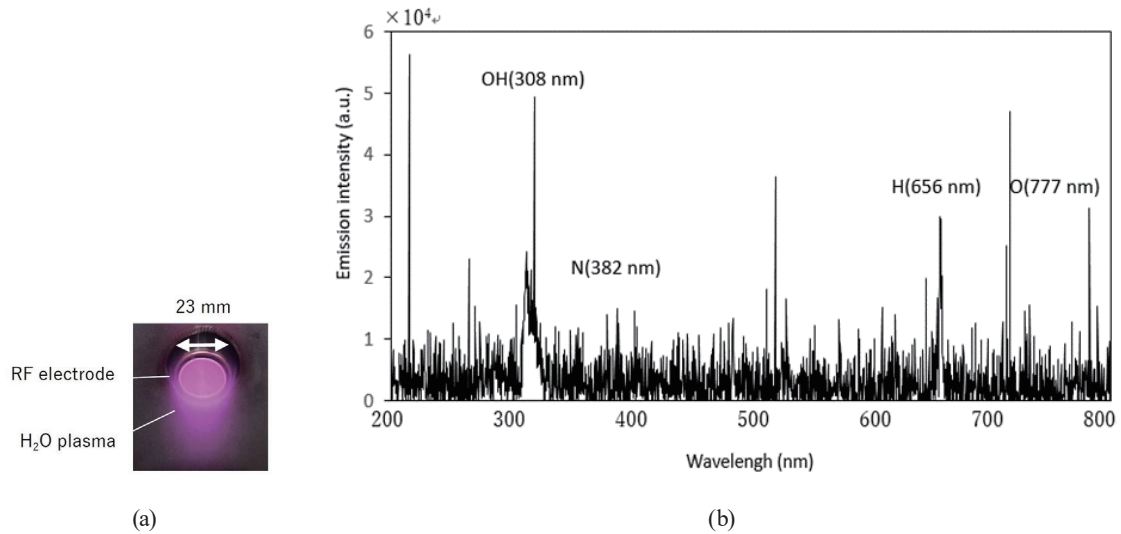


Fig. 2. (Color online) (a) Photograph of solid-source H<sub>2</sub>O plasma observed through the top quartz window. (b) Optical emission spectrum of H<sub>2</sub>O plasma observed through the top quartz window.

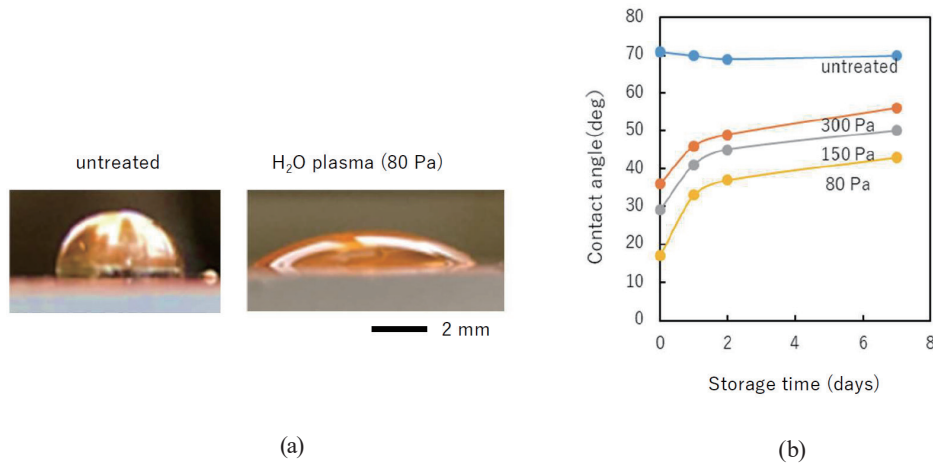


Fig. 3. (Color online) (a) Photographs of wetting of polyimide surface with a drop of pure water. (b) Contact angle of the polyimide surface as a function of storage time.

### 3.3 Deposition of Ge on polyimide surface

We deposited a Ge film with a thickness of 1055 nm on a polyimide sheet using a sputtering system (L-250S-FH, ANELVA). A thin Cr film (23 nm) was used to ensure a good contact between the Ge and the polyimide surface. The polyimide surface was subjected to plasma processing at a pressure of 1 Pa and an RF power of 100 W. Figure 4(a) shows the warpage angles of the Ge/polyimide sheet measured at 23 and 200 °C. The warpage of the sample was due to the difference in the thermal expansion coefficient between the polyimide and Ge. It was

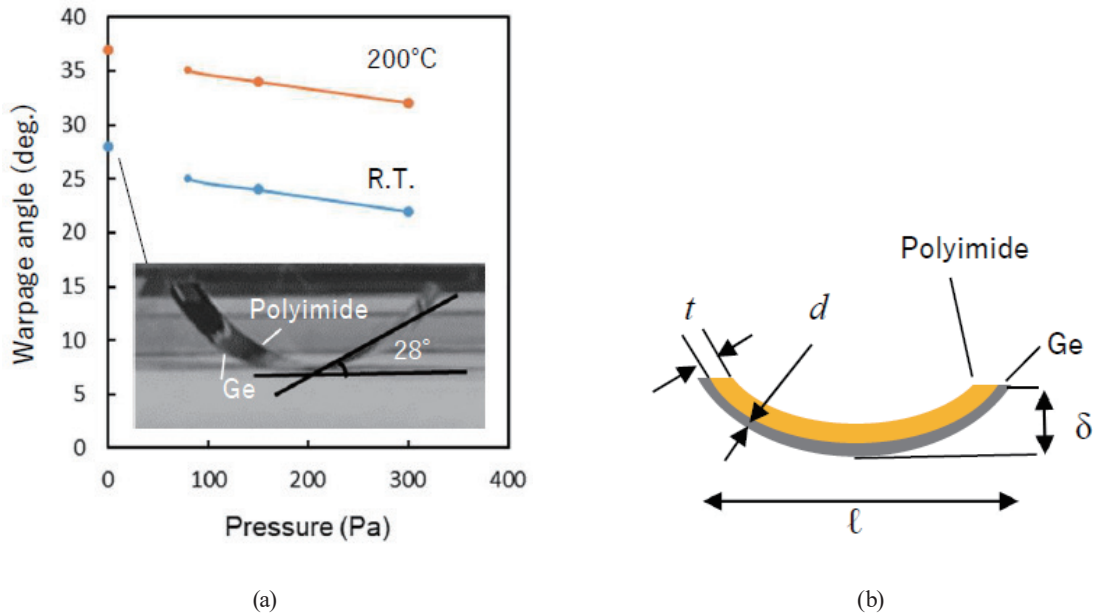


Fig. 4. (Color online) (a) Warpage angle of polyimide sheet with deposited Ge as a function of H<sub>2</sub>O plasma pressure. (b) Schematic of warpage of polyimide sheet with deposited Ge.

found that the warpage angle was reduced by plasma treatment at both temperatures, and the warpage angle decreased with increasing process pressure. The warpage angle at 200 °C was larger than that at 23 °C, although the trend in the decrease was almost the same at both temperatures. The internal stress in the rectangular substrate, as shown in Fig. 4(b), is expressed by

$$\sigma = \frac{Et \delta}{3(1-\nu)l d}, \quad (1)$$

where  $E$  is Young's modulus of the substrate,  $t$  is the thickness of the substrate,  $\nu$  is the Poisson ratio, and  $d$  is the thickness of the thin film.<sup>(24)</sup> Young's modulus of polyimide is 3 GPa and the Poisson ratio of Ge is 0.28. The compressive stress  $\sigma$  of the untreated sample at room temperature was estimated to be 77 MPa and that at a process pressure of 300 Pa was estimated to be 54 MPa. Therefore, the solid-source H<sub>2</sub>O plasma treatment reduced the internal stress in Ge deposited on a polyimide surface. Figures 5(a) and 5(b) respectively show the average roughness ( $Ra$ ) and AFM images of the polyimide surface and Ge surface as a function of the H<sub>2</sub>O plasma treatment pressure. The untreated polyimide surface was smooth with  $Ra$  of 0.01 nm.  $Ra$  of the Ge surface increased with increasing process pressure. The surface roughness of Ge deposited on the plasma-treated polyimide was less than that of Ge on the untreated sheet. We consider that Ge covered the roughness of the polyimide, which was increased by the plasma treatment, and, as a result,  $Ra$  of the Ge surface became less than that of the untreated polyimide sheet.

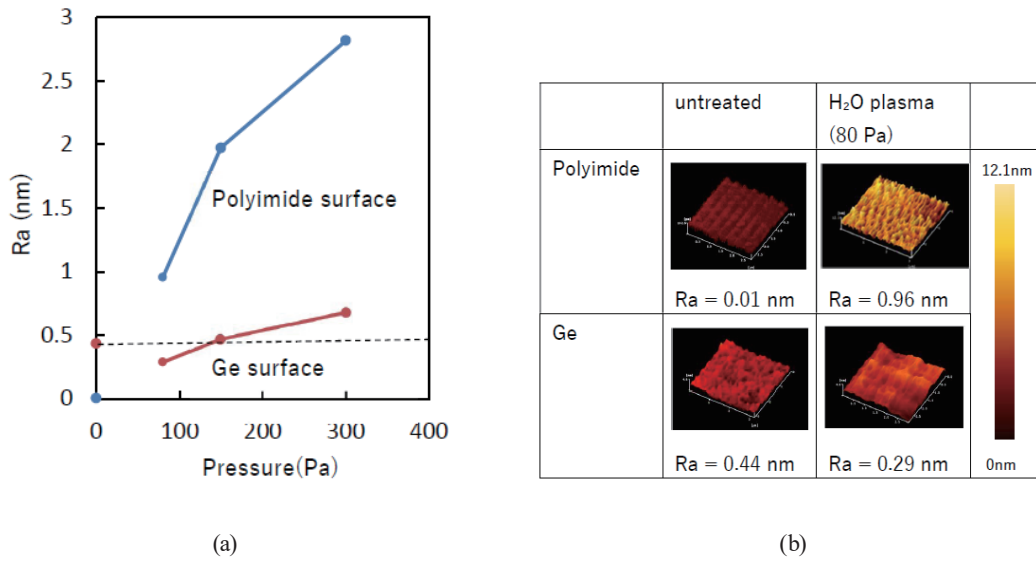


Fig. 5. (Color online) (a)  $R_a$  of polyimide surface and Ge surface as a function of  $H_2O$  plasma pressure. (b)  $3 \times 3 \mu m^2$  AFM images of polyimide surface and Ge surface before and after  $H_2O$  plasma treatment.

### 3.4 Bending tests of Ge film deposited on polyimide

We carried out bending tests of the Ge film deposited on polyimide to evaluate its applicability to flexible electrodes. The polyimide sheet with deposited Ge was put between 1-mm-thick stainless-steel plates to fix half side of the sample. Another side of the sample with the stainless-steel plate as a support was bent repeatedly to an angle of  $90^\circ$ . The radius of curvature was 2.5 mm. Figure 6(a) shows the sheet resistance measured by the four-probe method as a function of the number of bends. The sheet resistance increased with increasing number of bends. Figure 6(b) shows the crack depth of the surface as a function of the number of bends. The depths of the cracks and the intervals between them for the samples without plasma treatment were greater than those for the samples treated with  $H_2O$  plasma. The  $H_2O$ -plasma-treated sample has more cracks than the untreated sample. However, the depths of the cracks were much smaller than the Ge thickness. Therefore, the cracks have fewer electrical disadvantages, and the sheet resistance of the samples treated with  $H_2O$  plasma are lower than those of the samples without plasma treatment. From these results, we conclude that the contact at the interface between the polyimide treated with  $H_2O$  plasma and the Ge film was good and that the cracks remained shallow even when the polyimide was repeatedly bent.

### 3.5 Resistance of Ge electrode deposited on polyimide

Figure 7(a) shows a 559-nm-thick Ge electrode deposited on a 50- $\mu m$ -thick polyimide sheet. The width of the electrode was 100  $\mu m$  and its total length was 40 mm. Figure 7(b) shows the temperature dependence of the resistance of the Ge electrode measured with an electric tester (YX-361TR, Sanwa). The resistance was measured after holding for 30 min at the measurement



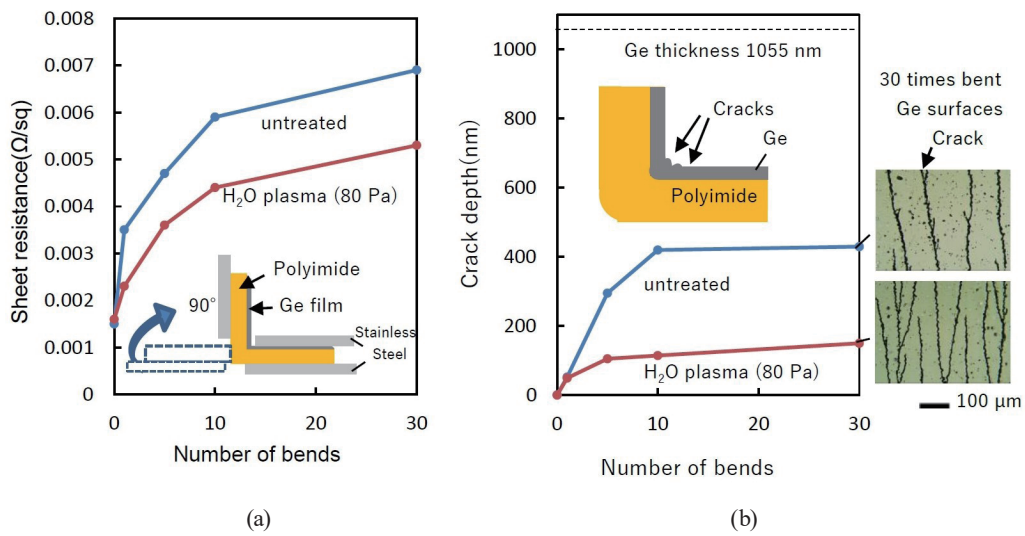


Fig. 6. (Color online) (a) Sheet resistance as a function of number of bends. (b) Crack depth as a function of number of bends.

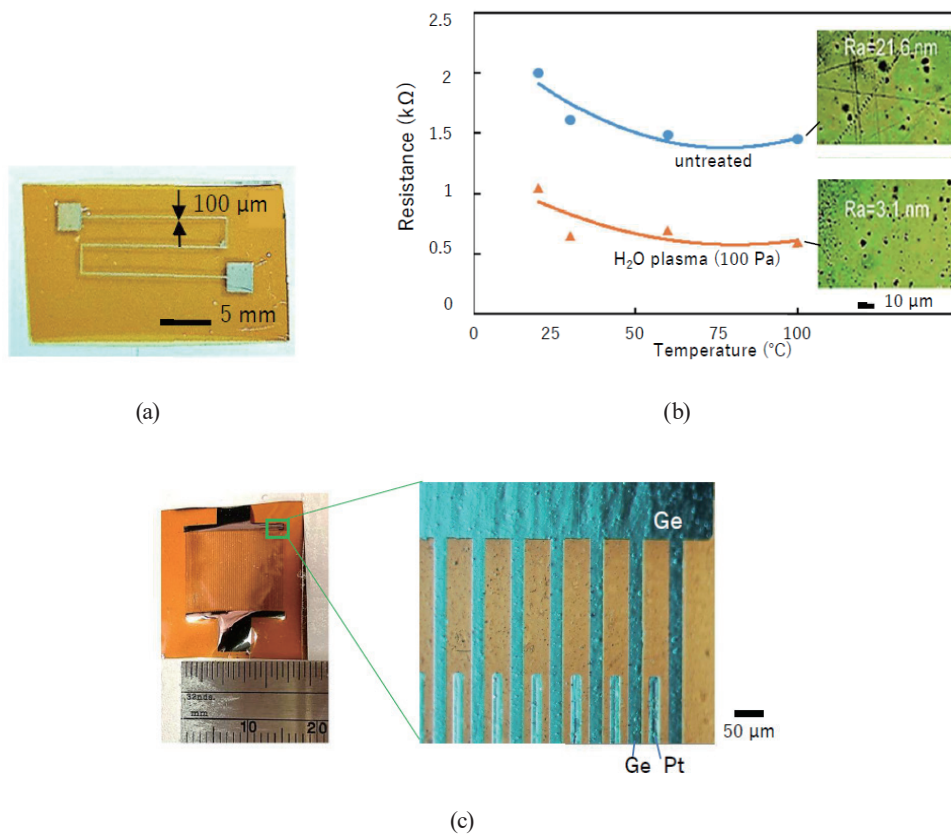


Fig. 7. (Color online) (a) Photograph of Ge electrode deposited on polyimide sheet. (b) Resistance of the Ge electrode deposited on the polyimide sheet as a function of temperature. (c) Photograph of fabricated comb-shaped Ge and Pt electrodes on polyimide sheet.

temperature. The resistance of the Ge electrode on polyimide both with and without plasma treatment decreased by the same tendency upon heating. These Ge electrodes are slightly warped, as shown in Fig. 4(a). However, these cracks caused by warpage, shown in Fig. 7(b) were smaller than the cracks, shown in Fig. 6(b), caused by the bending test. Therefore, these Ge electrodes were negligibly affected by warping, and the temperature characteristics of general intrinsic semiconductors were measured. The resistance of the electrode on polyimide treated with H<sub>2</sub>O plasma was approximately half that of the electrode without plasma treatment. In addition, the Ge surface on the untreated sample had more cracks than that on the plasma-treated sample and its *Ra* was also large. Therefore, we conclude that the increase in the resistance of the untreated sample is due to the cracks in the Ge electrode generated by the warpage of the polyimide sheet. As mentioned above, the H<sub>2</sub>O plasma treatment is effective for increasing the durability and decreasing the resistance of Ge electrodes on polyimide. Figure 7(c) shows comb-shaped Ge and Pt electrodes formed on a polyimide sheet treated with solid-source H<sub>2</sub>O plasma. The width of each electrode was 20 μm, the distance between the electrodes was 50 μm, and the number of combs was 142. Both Ge and Pt electrodes could be formed without disconnection. The performance of the device is under investigation.

#### 4. FTIR and XPS Analysis of Polyimide Surface Processed by Solid-Source H<sub>2</sub>O Plasma

We analyzed the polyimide surface treated by the solid-source H<sub>2</sub>O plasma by FTIR and XPS. Figure 8 shows the spectra of the polyimide surface measured by FTIR. In this experiment, we used samples processed for 5 min at a pressure of 100 Pa and an RF power of 10 W using the solid-source H<sub>2</sub>O plasma. These spectra were normalized by the peak intensity at 1500 cm<sup>-1</sup> for

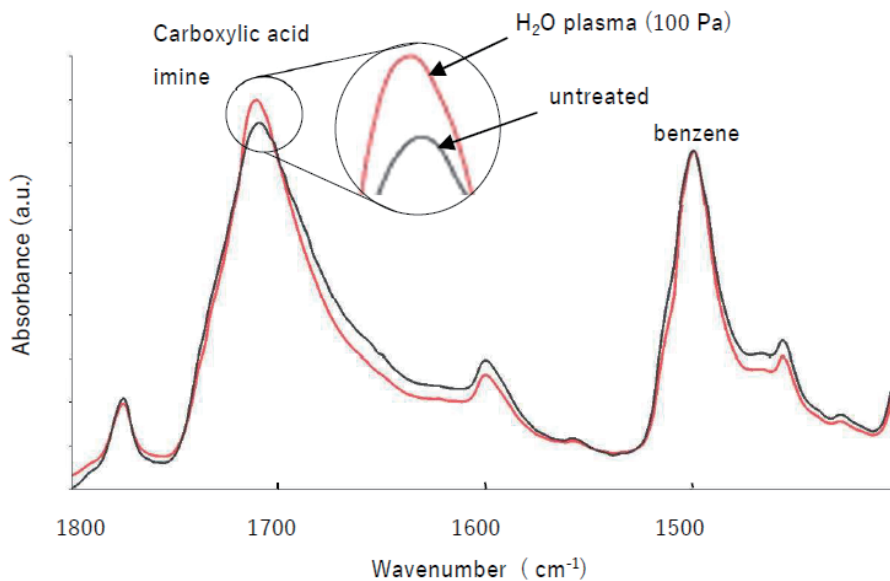


Fig. 8. (Color online) FTIR spectra of polyimide surface before and after H<sub>2</sub>O plasma (100 Pa) treatment.



benzene. The peak intensity of the polyimide surface treated with  $\text{H}_2\text{O}$  plasma increased at a wavenumber of  $1700\text{ cm}^{-1}$ . The peak at  $1700\text{ cm}^{-1}$  corresponds to carboxylic acids and imines.<sup>(25)</sup> On the basis of the results, we conclude that the imide rings were opened and that carboxylic acids and imines were generated by the  $\text{H}_2\text{O}$  plasma treatment.

Figure 9 shows C1s XPS spectra of the untreated and  $\text{H}_2\text{O}$ -plasma-treated polyimide surfaces. PHI MultiPak software (ULVAC-PHI) was used for peak separation of the spectra. In

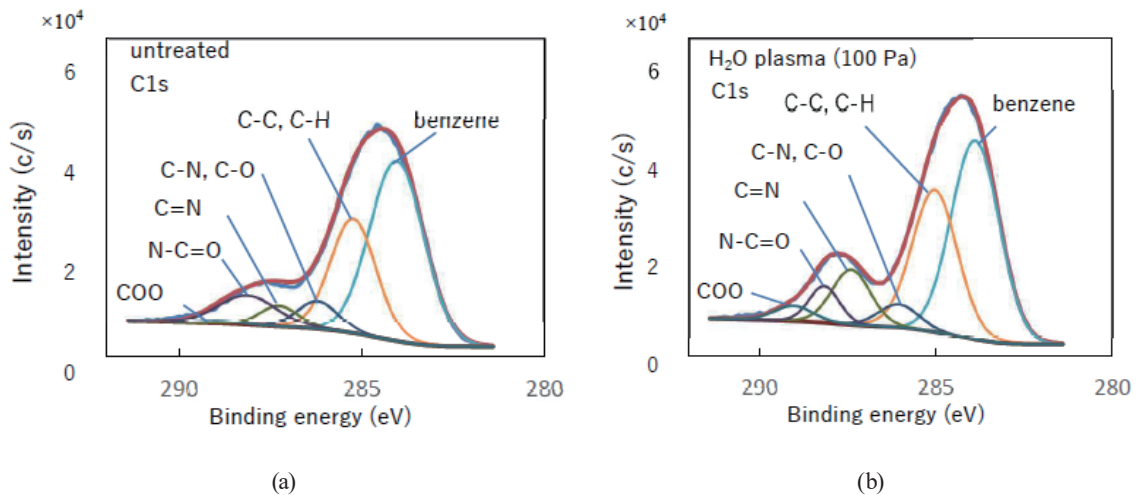


Fig. 9. (Color online) C1s XPS spectra of polyimide surface. (a) Untreated surface. (b) Surface treated with  $\text{H}_2\text{O}$  plasma (100 Pa).

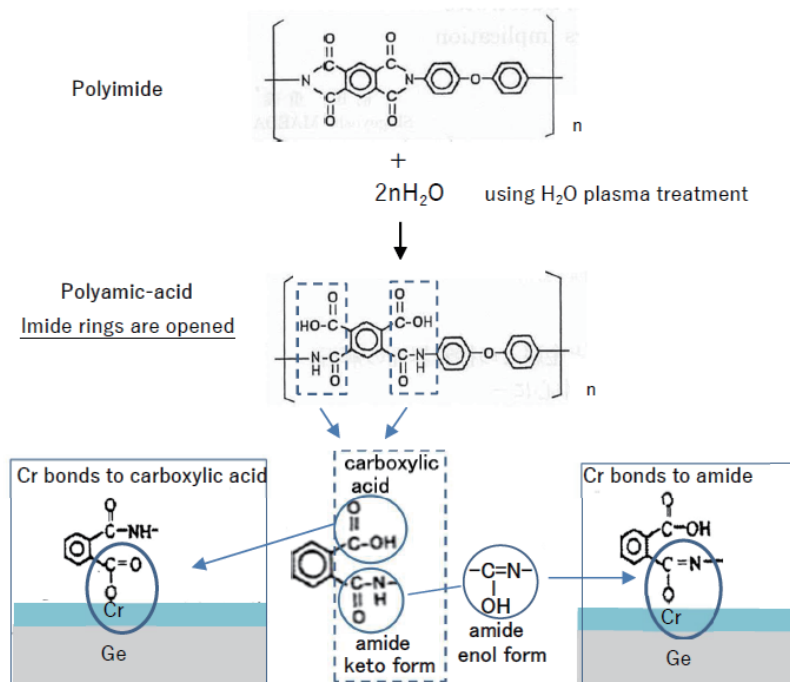


Fig. 10. (Color online) Model of chemical reaction and bonding mechanism on polyimide surface processed by  $\text{H}_2\text{O}$  plasma.

the spectra of C1s, the composition ratio of N–C=O bonds of imide was decreased from 9.7 to 4.1% and that of COO bonds was increased from 0.63% to 5.3% by the H<sub>2</sub>O plasma treatment. In addition, the composition ratio of C=N bonds was increased from 4.7 to 8.5% by the H<sub>2</sub>O plasma treatment.

Figure 10 shows a model of the chemical reaction and bonding mechanism of the polyimide surface processed by H<sub>2</sub>O plasma. A chemical reaction occurs whereby polyimide is converted to polyamic acid during the H<sub>2</sub>O plasma treatment. By this chemical reaction, we consider that the H<sub>2</sub>O plasma treatment opens the imide ring and increases the number of carboxylic acid and amide groups. When the amide group (–C(O)NH–) (keto form) is tautomerized to C(OH)=N bonds (enol form),<sup>(26)</sup> the number of C=N bonds increases. In other words, the increase in COO is considered to be due to the increase in the amount of carboxylic acid. Also, the increase in C=N is considered to be due to the increase in amide groups. This inference is consistent with the FTIR spectra shown in Fig. 8. Flament *et al.* proposed a model of O-bonding between a polyimide film formed by the thermal polymerization of polyamic acid and an Al surface.<sup>(27)</sup> In this model, some of the carboxyl and amide groups of polyamic acid are bonded to Al via O. We consider that the Cr adhesive layer in our experiment has a similar property to that of Al as it forms oxides at the interface. The first few monolayers of Cr may react with the pendant oxygen atoms in the polyamic acid, forming either Cr–oxygen complexes or Cr oxides at the interface.<sup>(28)</sup> We consider that the interface between the polyimide and Cr was bonded by the Cr–O–C bonds generated by the opening of the polyimide ring during H<sub>2</sub>O plasma treatment. We conclude that the roughness of the surface of the polyimide is increased by H<sub>2</sub>O plasma treatment, which increases the area of the adhesive interface, and that the many Cr–O–C bonds contribute to the improved adhesion.

## 5. Conclusions

We demonstrated that solid-source H<sub>2</sub>O plasma treatment is effective for the fabrication of Ge electrodes on a polyimide surface. By using a solid-source H<sub>2</sub>O plasma, the internal stress of a Ge-deposited polyimide sheet was decreased, and the adhesion between the polyimide and Ge was also improved. Moreover, the solid-source H<sub>2</sub>O plasma treatment was effective for increasing the bending durability and decreasing the resistance of the Ge electrode on the polyimide surface. We successfully fabricated a 142 line/space comb-shaped electrode with a width of 20 μm and a distance of 50 μm between the electrodes by applying the solid-source H<sub>2</sub>O plasma treatment. In addition, we deduced, from the results of XPS and FTIR analyses, that the interface between the polyimide and the Cr adhesive layer was bonded by Cr–O–C bonds generated by the opening of the polyimide ring during the solid-source H<sub>2</sub>O plasma treatment. We believe that the proposed solid-source H<sub>2</sub>O plasma process is useful for bonding polyimide and Ge in the fabrication of various electrodes, such as flexible semiconductor electrodes.

## Acknowledgments

We thank Ms. T. Kanai of Tokyo Institute of Technology for performing the XPS analysis. This work was supported by JSPS KAKENHI(B) (21H02041) and the Core Facility Program (JPMXS0440200021).

## References

- 1 J. B. Park, J. S. Oh, E. L. Gil, S. J. Kyoung, J. T. Lim, and G. Y. Yeom: *Electrochem. Soc.* **157** (2010) 614.
- 2 K. Ito: *J. Faculty of Engineering, Shinshu University* **23** (1967) 97 (in Japanese).
- 3 J.-H. Park, K. Kasahara, K. Hayama, M. Miyao, and T. Sadoh: *Appl. Phys. Lett.* **104** (2014) 252110.
- 4 M. Shiratani, S. Tanami, D. Sakamoto, H. Chou, H. Seo, D. Yamashita, N. Inagaki, and K. Koga: *Proc. 64th JSAP Spring* (2017) 07-126 (in Japanese).
- 5 M. Maeda: *Electrochem. Soc.* **29** (1961) 8 (in Japanese).
- 6 H. Kohata, B. Mei, Y. Wang, K. Mizukoshi, T. Isobe, A. Nakajima, and S. Matsusita: *Energy Fuels* **36** (2022) 11619.
- 7 S. Matsushita, T. Araki, B. Mei, S. Sugawara, Y. Inagawa, J. Nishiyama, T. Isobe, and A. Nakajima: *J. Mater. Chem. A* **7** (2019) 18249.
- 8 Y. Imai: *Recent Progress of Polyimide* (2002) (in Japanese). [http://fibertech.or.jp/JPIC/pdf/2002\\_01.pdf](http://fibertech.or.jp/JPIC/pdf/2002_01.pdf)
- 9 S. H. Kim, S. W. Na, N.-E. Lee, Y. W. Nam, and Y. H. Kim: *Surf. Coat. Technol.* **200** (2005) 2072.
- 10 S. H. Kim, S. H. Cho, N.-E. Lee, H. M. Kim, Y. W. Nam, and Y. H. Kim: *Surf. Coat. Technol.* **193** (2005) 101.
- 11 A. K. S. Ang, E. T. Kang, K. G. Neoh, K. L. Tan, C. Q. Cui, and B. T. Lim: *Polymer* **41** (2000) 489.
- 12 A. Weber, A. Dietz, R. Pockelmann, and C. P. Klages: *Electrochem. Soc.* **3** (1997) 1131.
- 13 B. Chapman: *Glow Discharge Processes* (John Wiley and Sons, New York, 1980) p. 432.
- 14 S. R. Holmes-Farley, R. H. Reamey, T. J. McCarthy, J. Deutch, and G. M. Whitesides: *Langmuir* **1** (1985) 725.
- 15 A. J. Dias and T. J. McCarthy: *ACS Macromol.* **18** (1985) 1826.
- 16 C. A. Costello and T. J. McCarthy: *ACS Macromol.* **20** (1987) 2819.
- 17 K. Lee and T. J. McCarthy: *ACS Macromol.* **21** (1988) 309.
- 18 K. Lee and T. J. McCarthy: *ACS Macromol.* **21** (1988) 2318.
- 19 K. Lee, S. P. Kowalczyk, and J. M. Shaw: *ACS Macromolecules* **23** (1990) 2097.
- 20 K. Fatyeyeva, A. Dahi, C. Chappay, D. Langevin, J.-M. Valleton, F. Poncin-Epaillard, and S. Marais: *RSC Adv.* **4** (2014) 31036.
- 21 H. Terai, R. Funahashi, T. Hashimoto, and M. Kakuta: *IEEJ Trans. Sens. Micromach.* **138** (2018) 358 (in Japanese).
- 22 M. Tohnishi and A. Matsutani: *Proc. 69th JSAP Spring* (2022) 01-013 (in Japanese).
- 23 M. Tohnishi and A. Matsutani: *Sens. Mater.* **33** (2021) 569.
- 24 D. W. Hoffman: *Phys. Thin Films* **3** (1933) 211.
- 25 N. B. Colthup: *J. Opt. Soc. Am* **40** (1950) 397.
- 26 S. Maeda: *J. Soc. Colour Mater.* **78** (2005) 131 (in Japanese).
- 27 O. Flament, J. Russat, and F. Druet: *J. Adhes. Sci. Technol.* **4** (1990) 109.
- 28 N. J. Chou, D. W. Dong, J. Kim, and A. C. Liu: *J. Electrochem. Soc.* **131** (1984) 2335.

